Chapter III

3 Electrodeposition of Zinc Nickel Alloy

Advances in electroplating technology since the mid-1970 have enabled a range of zinc alloy coatings to be deposited with a bright appearance, consistent surface finish, and uniform thickness. In particular, the binary zinc alloys formed with nickel have been developed as corrosion resistant coatings containing 10 wt% to 18wt% Ni are used. It has been established that, although the barrier properties of zinc coatings are improved progressively by the addition of nickel, this effect is accompanied by a gradual reduction in the ability to protect steel sacrificially as the nickel level is raised. A recent study showed that the nickel content for electrodeposited zinc alloys in saline environments can be increased to ≈ 26 wt% before the coating cease to behave sacrificially toward steel [78]. In the present work, the effect of agitation during the deposition was evaluated. Two different modes of agitation, air agitation and sonication are experimented to understand the basic changes, which can be brought out in the coating and in the overall process is studied. Following are the results obtained from the two methods.

3.1 X-ray analysis

Figure 3.1 and 3.2 shows the diffractograms of the co-deposits of zinc and nickel obtained under air-agitated and sonicated conditions respectively. The diffractograms were plotted in the order of decreasing current density; obtained at 5A/dm^2, next 4A/dm^2 and so on.

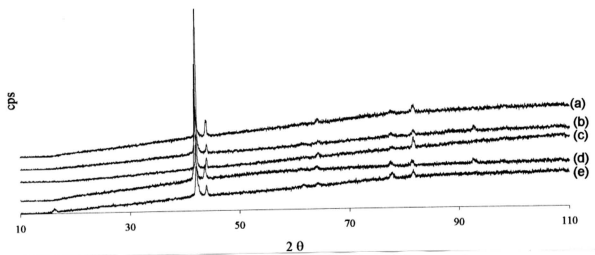

Figure 3.1 X-ray diffractogram of the deposit obtained at various plating current densities under air agitated conditions
(a) current Density = 5A/dm^2
(b) current Density = 4A/dm^2
(c) current Density = 3A/dm^2
(d) current Density = 2A/dm^2
(e) current Density = 1A/dm^2

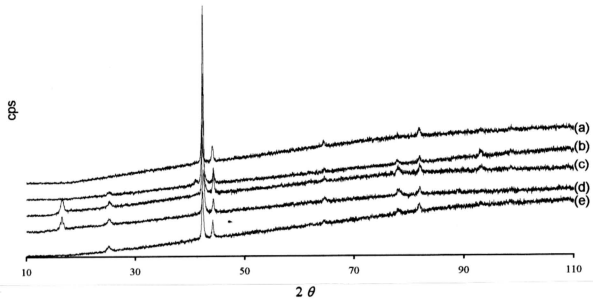

Figure 3.2 X-ray diffractogram of the deposit obtained at various plating current densities under sonicated conditions

(a) current Density = 5A/dm^2
(b) current Density = 4A/dm^2
(c) current Density = 3A/dm^2
(d) current Density = 2A/dm^2
(e) current Density = 1A/dm^2

The highest reflection intensity for air-agitated deposits appears between 41.7° to 42.07°. In all cases, there is a gradual increase in the intensity with plating current density. In the case of the sonicated batch, appearance of the highest reflection intensity occurs in between 42.14° to 42.42°. In this case also a gradual increase in the intensity with plating current density can be observed. It should be noted that there is a small shift in the position of the peak of highest reflection intensity when the air-agitated and the sonicated batch X-ray diffractograms are compared. In both cases it could be observed with increase in plating current density the peak intensity increases showing the increase in crystalline nature.

The major difference in the diffractograms is the appearance of the peak at 25.18° in sonicated batch. However, it can be observed that with increase in plating current density, the peak (25.18°) intensity of sonicated batch decreases; and at a plating current density of 5 A/dm^2 this peak vanishes and the diffraction looks similar to that of the air-agitated batch. Thus the appearance of this particular peak indicates a different mode of crystal growth in sonicated batches. When the diffractograms of those deposits from air-agitated batches were compared with that of standard zinc metal's, the highest reflection intensity of the standard zinc metal matches with that of the second highest reflection intensity deposit (Table 3.1). In the case of the sonicated batches, no such peak could be observed at the highest reflection intensity position of the zinc metal (Table 3.2). As a further investigation, the diffractogram of mild steel (substrate) is compared with those of the sonicated deposits. In this case the highest reflection intensity of mild steel matches with the second highest reflection intensity of the deposit. From these observations it could be said that deposition assisted by air agitation leads to heterogeneous codeposition of the two metals, where as deposition assisted by sonication leads to homogenous codeposition. The crystallinity of the deposits obtained by these two different methods varies. Figures 3.3 and 3.4 shows the diffractograms of the deposits obtained under sonicated and air-agitated conditions respectively and the comparison with standard zinc.

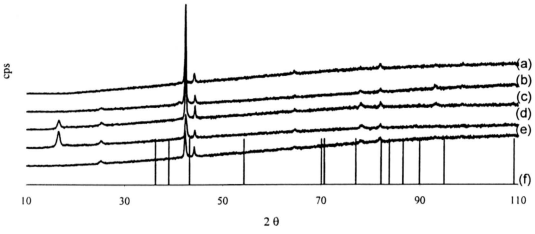

Figure 3.3 Comparison of the X-ray diffractogram of the deposit obtained at various plating current densities under sonicated condition with X-ray diffractogram of standard zinc metal

(a) current Density = 5A/dm^2
(b) current Density = 4A/dm^2
(c) current Density = 3A/dm^2
(d) current Density = 2A/dm^2
(e) current Density = 1A/dm^2
(f) standard zinc metal

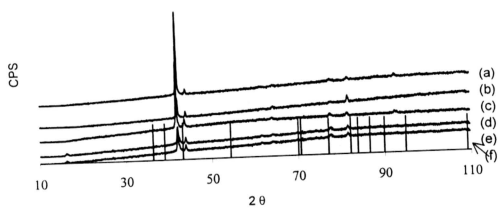

Figure 3.4 Comparison of the X-ray diffractogram of the deposit obtained at various plating current densities under air agitated conditions with X-ray diffractogram of standard zinc metal

(a) current Density = 5A/dm^2
(b) current Density = 4A/dm^2
(c) current Density = 3A/dm^2
(d) current Density = 2A/dm^2
(e) current Density = 1A/dm^2
(f) standard zinc metal

Following Tables 3.1 and 3.2 give the observed highest reflection intensity of the diffractograms of air-agitated and sonicated batches and that of the mild steel (substrate) and zinc standards respectively.

Table 3.1 Comparison of the highest reflection intensity peak position of mild steel (substrate), zinc and to that of deposit obtained under air-agitated condition.

Plating current density	Highest Reflection Intensity peak position (θ) of deposit	Highest Reflection Intensity peak position (θ) of	
		Mild steel (substrate)	Zinc (standard)
1 A/dm^2	43.95	44.31	43.87
2 A/dm^2	43.63		
3 A/dm^2	43.96		
4 A/dm^2	43.96		
5 A/dm^2	43.82		

Table 3.2 Comparison of the highest reflection intensity peak position of mild steel (substrate), zinc and to that of deposit obtained under sonicated condition.

Plating current density	Highest Reflection Intensity peak position (θ) of deposit	Highest Reflection Intensity peak position (θ) of	
		Mild steel (substrate)	Zinc (standard)
1 A/dm2	44.19	44.31	43.87
2 A/dm2	44.27		
3 A/dm2	44.31		
4 A/dm2	44.28		
5 A/dm2	44.08		

Studies [78] on pyrometallurgically prepared zinc-nickel alloy and electrodeposited zinc-nickel show similar intermediate phases. Lihil [79] reported the phase ranges at 250°C indicating that 10 to 25% of zinc content in the alloy results in α form of alloy, 45-55% of zinc results in β' form of alloy. Elaborate study done by Brenner [9] reported the more complete equilibrium phase compositions at 200°C, indicating the presence of various phases of the zinc-nickel alloy apart from α and β'. He also reported various other equilibrium phases of zinc-nickel alloy (like $\alpha+\beta'$, $\gamma'+\beta'$, $\delta+\eta$, $\gamma'+\gamma$, $\gamma+\delta$). R. Noumi et.al. [80] work on three electrodeposits from sulfate baths using x-ray diffraction and electron probe microanalysis showed that nickel and zinc were homogeneously distributed without evidence of segregation. Ramachar and Panikkar [81] reported on five more phases of electrodeposited zinc-nickel alloy. In the following Figures 3.5 to 3.8 X-ray diffractograms of deposits obtained from air-agitated batches were compared with X-ray diffractograms various intermettalic standard compounds of zinc and nickel. From the comparison, it can be observed that the pattern does not match with the standard compounds.

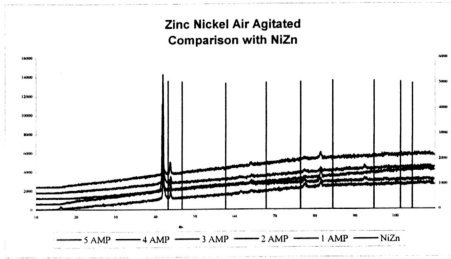

Figure 3.5 Comparison of X-ray diffractograms of the deposits of Zinc-Nickel obtained under air agitated condition with NiZn

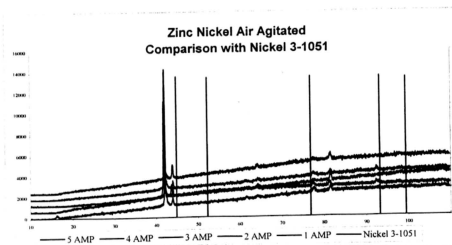

Figure 3.6 Comparison of X-ray diffractograms of the deposits of Zinc-Nickel obtained under air agitated condition with Ni3-1051

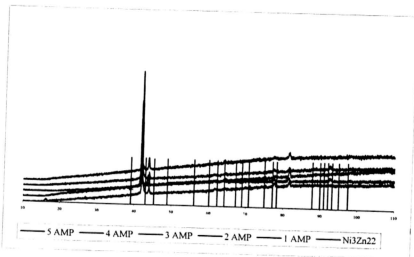

Figure 3.7 Comparison of X-ray diffractograms of the deposits of Zinc-Nickel obtained under air agitated condition with Ni_3Zn_{22}

Figures 3.9 to 3.11 show the comparison of the diffractograms of the sonicated samples with those of the thermally prepared intermetallic compounds of zinc and nickel. In this case also no similarity could be observed. These observations lead to the conclusion that the deposits obtained under present study are not same as those of intermetallic compounds. It is also apparent that the plating under sonicated condition follows a different crystal growth kinetics.

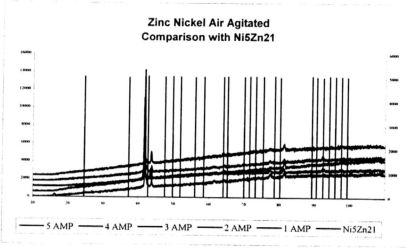

Figure 3.8 Comparison of X-ray diffractograms of the deposits of Zinc-Nickel obtained under air agitated condition with Ni_5Zn_{21}

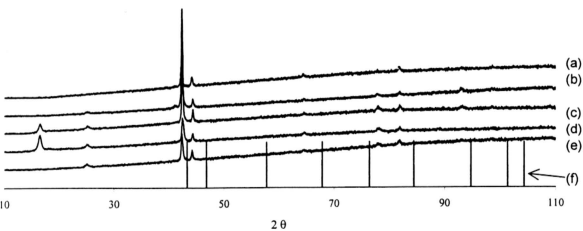

Figure 3.9 Comparisonof X-ray diffractograms of deposits obtained under sonicated condition and the intermetallic compound ZnNi. Straight line are that of the standard.

(a) current density = 5 A/dm^2
(b) current density = 4 A/dm^2
(c) current density = 3 A/dm^2
(d) current density = 2 A/dm^2
(e) current density = 1 A/dm^2
(f) ZnNi-standard intermetallic compound of Zinc and nickel

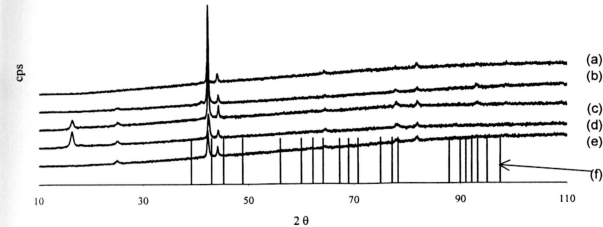

Figure 3.10 Comparisonof X-ray diffractograms of deposits obtained under sonicated condition and the intermetallic compound Ni_3Zn_{22}. Straight line are that of the standard.

(a) current density = 5 A/dm^2
(b) current density = 4 A/dm^2
(c) current density = 3 A/dm^2
(d) current density = 2 A/dm^2
(e) current density = 1 A/dm^2
(f) Ni_3Zn_{22}-standard intermetallic compound of Zinc and nickel

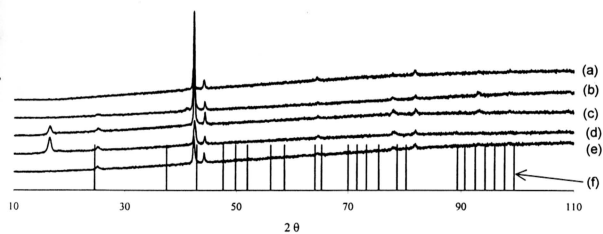

Figure 3.11 Comparisonof X-ray diffractograms of deposits obtained under sonicated condition and the intermetallic compound Ni_5Zn_{21}. Straight line are that of the standard.

(a) current density = 5 A/dm^2
(b) current density = 4 A/dm^2
(c) current density = 3 A/dm^2
(d) current density = 2 A/dm^2
(e) current density = 1 A/dm^2
(f) Ni_5Zn_{21}-standard intermetallic compound of Zinc and nickel

Cluster sizes of the deposit were calculated using the data obtained from the X-ray diffractogram, using the formula

$$D = \frac{0.9\lambda}{W\cos\theta} \quad (1)$$

where D is the diameter of the cluster in angstroms, λ is the wavelength of the X-ray source, W is the width of the peak, θ is the angle at which the peak appears. Calculated cluster sizes values of both sonicated and air-agitated electrodeposits are tabulated in Table 3.3

Table 3.3 Cluster size for electrodeposits assisted by sonication and air agitation

Current A/dm2	Cluster size in Angstroms	
	Sonicated	Air-agitated
1	817.03	589.63
2	653.60	828.00
3	601.55	852.69
4	719.72	689.04
5	445.35	712.67

Calculated values of cluster size show a decrease in cluster size for the sonicated deposition and an increase in the cluster size for the air-agitated deposition. It is known that at high plating current densities i.e. at

high rates of deposition whisker formation is more favored than continuos deposition. Whiskers are less adherent compared to the continuos coating. Figure 3.12 show the variation of cluster size with plating current density for zinc nickel deposits obtained under sonicated conditions.

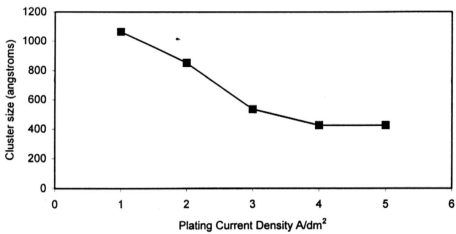

Figure 3.12 Variation of cluster size with plating current density calculated from XRD data for the zinc nickel deposits obtained under sonicated condition

From figure 3.12, it is evident that plating under sonication affects the nucleation or the crystal growth. It happens in the reverse order for the air-agitated deposits in which, the cluster size increases with increase in plating current density. Figure 3.13 shows the variation in cluster size with current density for the zinc nickel deposit under air agitation. This decrease in cluster size for the sonicated batches could be because of the high frequency mechanical vibrations imposed over the deposit. X-ray diffractogram alone is not sufficient to give the reason for the difference in

the behavior of the two different mode of deposition. Thus letting it possible for materials getting coated in a compact fashion rather than the loose and less adherent bulk or big particles.

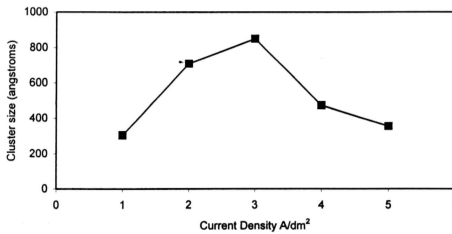

Figure 3.13 Variation of cluster size with plating current density calculated from XRD data for the zinc nickel deposits obtained under air agitated condition

3.2 EDAX ANALYSIS

Elemental composition is another factor, which determines the performance of the coating against corrosion. Hence as discussed in Chapter II EDAX analysis were done on both the deposits and the results and observation are as follows.

Table 3.4 and 3.5 show the EDAX results of the zinc nickel alloy deposited under air agitation and sonication respectively (Ref. Appendix for the figures ZNA1-ZNA5, ZNS1-ZNS5)

Table 3.4 EDAX results of zinc-nickel deposit under air Agitation

Current A/dm^2	Element % of Ni	Element % of Zn
1	10.04	89.96
2	9.78	90.22
3	7.68	92.32
4	8.79	91.21
5	8.8	91.2

Table 3.5 EDAX results of zinc-nickel deposit under sonication

Current A/dm^2	Element % of Ni	Element % of Zn
1	12.09	87.91
2	12.12	87.88
3	10.44	89.56
4	10.14	89.86
5	9.66	90.34

The plating current density and less-noble metal concentration curve [82] as shown in Figure 3.14 shows both the processes are of

anomalous co-deposition. Transition current lies between 2 and 3 A/dm^2 for both air-agitated and sonicated method. The trend of the curve after entering region II (Figure 1.3) changes and by sonication more or less a plateau region can be seen, where as by air agitation the concentration tends to increase and then decrease at high plating current density. Also the concentration of the noble metal is high with air agitation as compared to that of sonication.

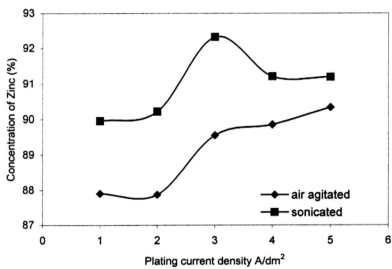

Figure 3.14 Plating current density versus zinc metal concentration in the deposit for the zinc nickel deposits obtained under both air agitated and sonicated condition

Figure 3.14 shows the element percentage of zinc in the deposit and Figure 3.15 shows the element percentage of nickel. By air agitation concentration of nickel obtained in the coating was less compared to the concentration of nickel in deposits under sonication. This could be

because of the degree of agitation delivered by sonication, resulting in maximizing the diffusion of the metal ions at or near the cathode area. It is evident from Figure 3.15 that sonication helps in attaining high

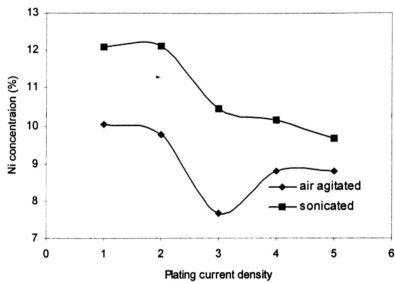

concentration of nickel in the deposit, the optimum concentration of nickel can be obtained at current density of 3 A/dm^2.

Figure 3.15 Plating current density versus nickel metal concentration in the deposit for the zinc nickel deposits obtained under both air agitated and sonicated condition

Nucleation studies done by Yu-Po Lin [83] indicates that at the initial stages of deposition, nickel and zinc nucleation and growth are influenced by the kinetics of the reacting ion reduction process at the interface of substrate and solution, and also by the character of hydrogen adsorption/desorption on the substrate. Weak adsorption results in high

concentration of nickel, which is in accordance with the high concentration of nickel as shown in Figure 3.15.

3.3 SEM Analysis

Figures 3.16 to 3.20 shows the SEM micrographs of deposits obtained under air-agitated condition. Figures 3.21 to 3.25 shows the SEM micrographs of deposits obtained under sonicated conditions.

Scanning micrograph of the deposit obtained at $1 A/dm^2$ under air-agitated condition (Figure 3.16) shows that the deposit is more clustered and it lacks any particular crystal shape [nodular appearance as reported by R. Alabalat et.al. [84] even at a magnification of 10,000 factors, though the deposit is crystalline as shown by the X-ray diffractogram Figure 3.1.

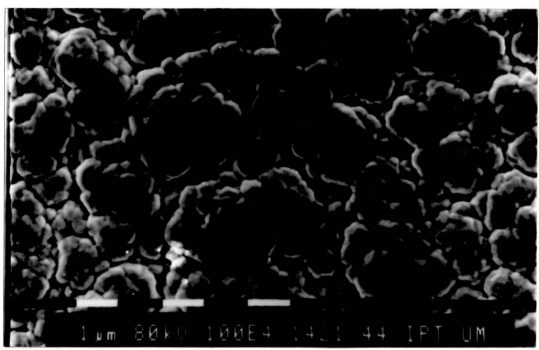

Figure 3.16 SEM micrograph of the Zinc-Nickel obtained under air-agitated condition at 1 A/dm^2

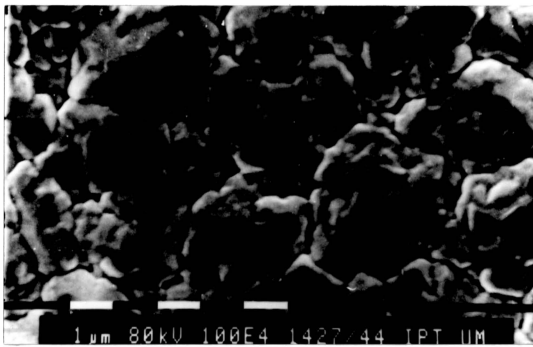

Figure 3.17 SEM micrograph of the Zinc-Nickel obtained under air-agitated condition at 2 A/dm^2

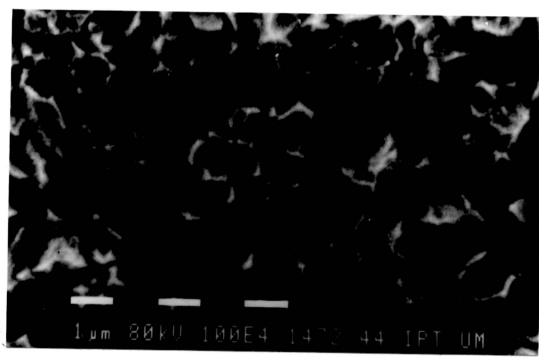

Figure 3.18 SEM micrograph of the Zinc-Nickel obtained under air-agitated condition at 3 A/dm^2

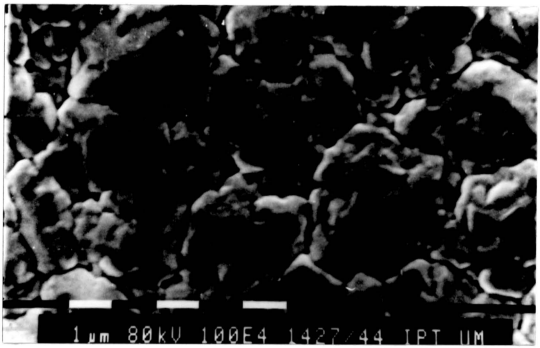

Figure 3.17 SEM micrograph of the Zinc-Nickel obtained under air-agitated condition at 2 A/dm^2

Figure 3.18 SEM micrograph of the Zinc-Nickel obtained under air-agitated condition at 3 A/dm^2

Figure 3.19 SEM micrograph of the Zinc-Nickel obtained under air-agitated condition at 4 A/dm^2

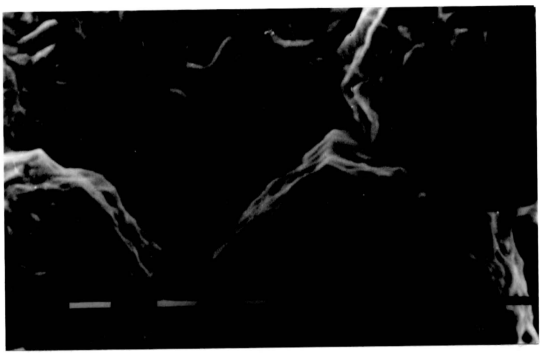

Figure 3.20 SEM micrograph of the Zinc-Nickel obtained under air-agitated condition at 5 A/dm^2

While the SEM micrograph of the coating obtained at $2 A/dm^2$ shows reduced cluster size and the crystal faces becomes apparent as observed in figure 3.17. This trend continues with increasing plating current density and it can be observed in the figures 3.18, 3.19, 3.20. Distribution of the particle size also become narrower with increase in plating current density, but this trend is not in accordance with the cluster size calculation done using the X-ray diffractogram. This difference could be because, the peak width values used in the formula depends on the purity of the crystal, and the purer the crystal the narrower the peak width will be.

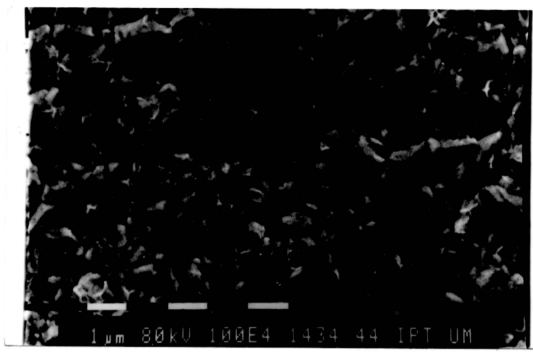

Figure 3.20 SEM micrograph of the Zinc-Nickel obtained under sonicated condition at 1 A/dm^2

Figure 3.21 SEM micrograph of the Zinc-Nickel obtained under sonicated condition at 2 A/dm^2

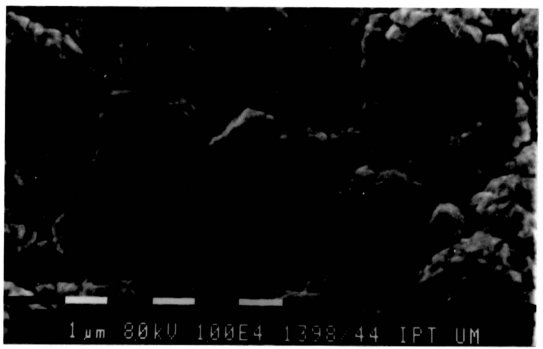

Figure 3.23 SEM micrograph of the Zinc-Nickel obtained under sonicated condition at 3 A/dm^2

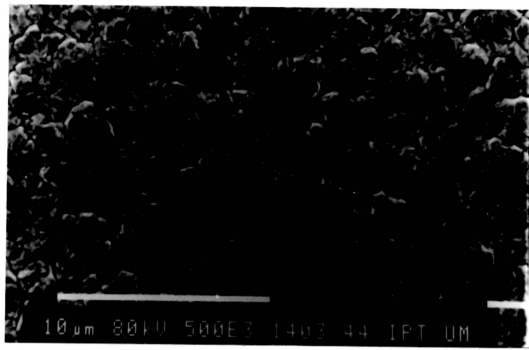

Figure 3.24 SEM micrograph of the Zinc-Nickel obtained under sonicated condition at 4 A/dm^2

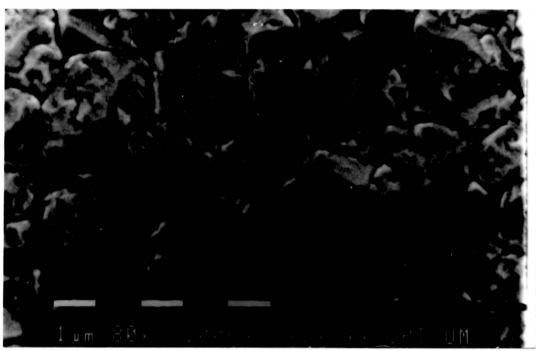

Figure 3.25 SEM micrograph of the Zinc-Nickel obtained under sonicated condition at 5 A/dm^2

Figure 3.26 shows the variation of peak width of the highest reflection intensity of the deposit obtained under air-agitated condition. It can be seen that the peak width decreases with increase in current density until $3\,A/dm^2$ and after that there is a increase in the peak width. This indicates the decrease in the purity of the crystals thus obtained, and hence there is a change in the cluster size values.

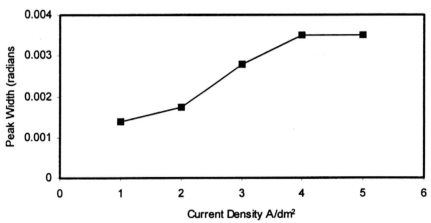

Figure 3.26 Peak width variation of the peak with highest reflection Intensity for Zinc-Nickel deposits obtained under sonicated condition.

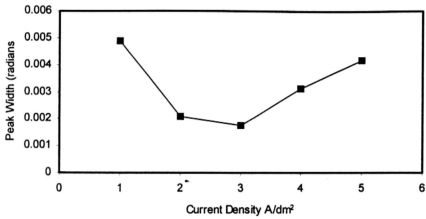

Figure 3.27 Peak width variation of the peak with highest reflection Intensity for Zinc-Nickel deposits obtained air-agitated condition.

It was reported by Ramadan et.al.[85] that the grains usually gives larger size (from SEM) than those determined by X-ray broadening, probably because the coherent diffraction domains are smaller than the average size according to direct observation. Scanning micrographs of the deposits obtained at $1 A/dm^2$ under sonicated condition shows (figure 3.21) an even distribution of the particle size with definite faces unlike the one obtained under air-agitated condition. With increase in plating current density the particle size increases and crystal face becomes apparent. Similar to the SEM micrographs of the air-agitated deposits, sonicated deposits also shows discrepancies in the cluster size (calculated values). Figure 3.27 shows the variation in the cluster size and the peak width for the sonicated deposits. Unlike the deposits obtained under air-agitated

condition sonicated deposits show a gradual increase in the peak width, that is purity of the crystal decreases with increasing plating current.

3.4 AFM results

Figures 3.28 to 3.32 shows the AFM scans of the deposits obtained under air-agitated conditions. Figure 3.28 shows the morphology of the deposit obtained at $1A/dm^2$ under agitated condition, the peak to base height is at a maximum indicating the deposit is coarse and uneven coating. Also the individual clusters or nodules had attained a pillar like structure and its being almost vertical. Thus the coating is more towards cluster formation rather than being a continuos. Figure 3.29 shows the morphology of the coating obtained at plating current density of $2A/dm^2$. In this case also the coating is more clustered but it should be noted that the distance between the neighboring clusters is much reduced. This trend continues and at a plating current density of $5A/dm^2$ the coating is even and smooth. As discussed in section 3.3 SEM analysis in figures 3.21 to 3.25, it can be seen that the deposits obtained under air-agitated condition results in a deposit of high degree of crystalinity. AFM scan reveals the same, as shown in the figures 3.33 to 3.37 for the scans of deposits obtained under sonicated condition. It should be noted that the deposit obtained under this condition yields a coating of more uniform surface. Though the deposit is smoother and the cluster size is smaller when compared to the air-agitated deposits it is

worth while to note the missing finer grain structures in the sonicated deposits.

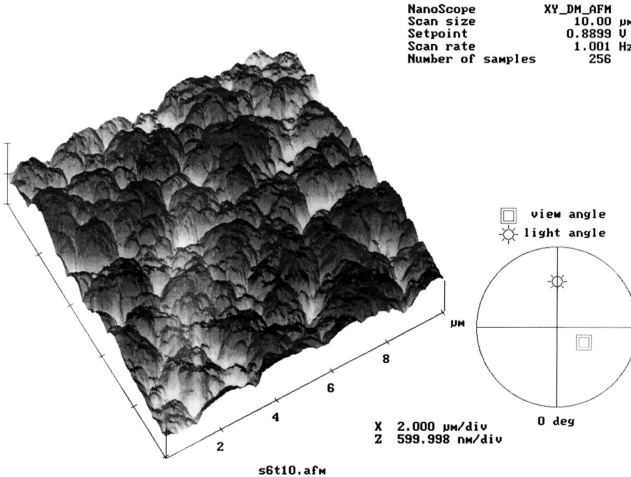

Figure 3.28 AFM scan of Zinc-Nickel deposit obtained under air agitated condition [plating current density = 1 A/dm^2]

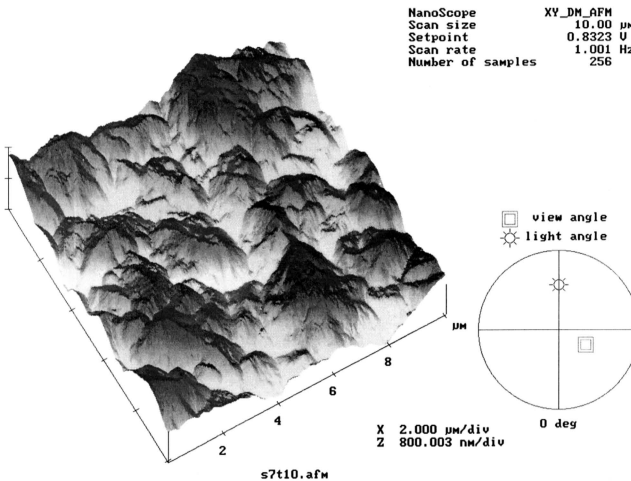

Figure 3.29 AFM scan of Zinc-Nickel deposit obtained under air agitated condition [plating current density = 2 A/dm^2]

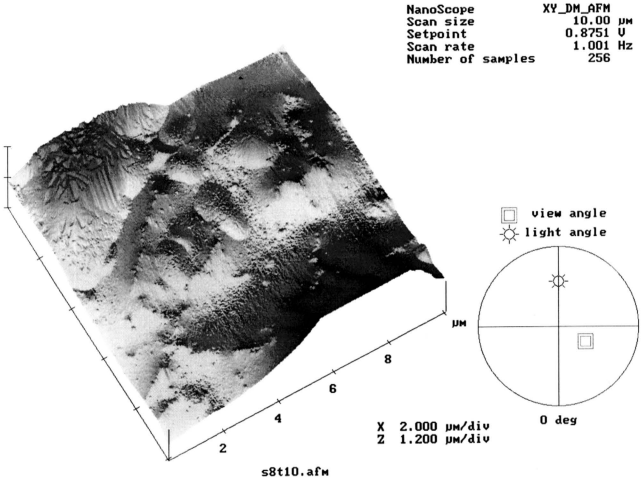

Figure 3.30 AFM scan of Zinc-Nickel deposit obtained under air agitated condition [plating current density = 3 A/dm^2]

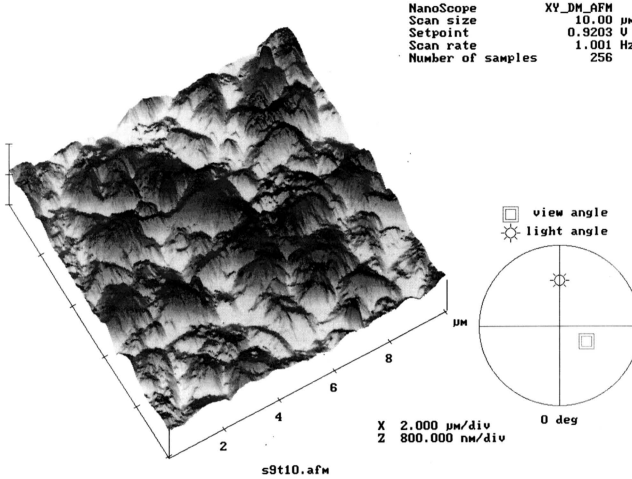

Figure 3.31 AFM scan of Zinc-Nickel deposit obtained under air agitated condition [plating current density = 4 A/dm^2]

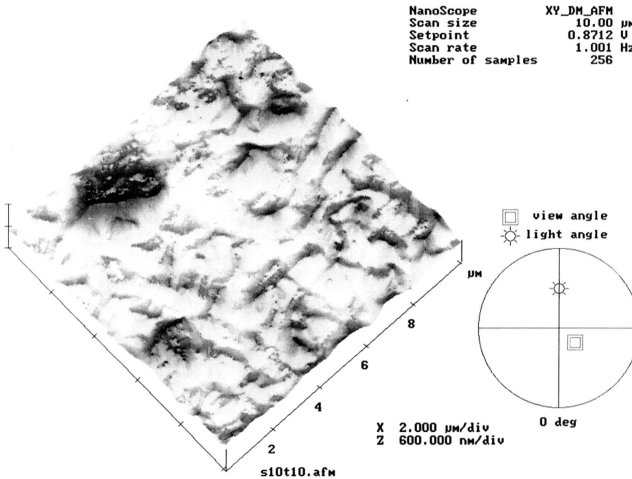

Figure 3.32 AFM scan of Zinc-Nickel deposit obtained under air agitated condition [plating current density = 5 A/dm^2]

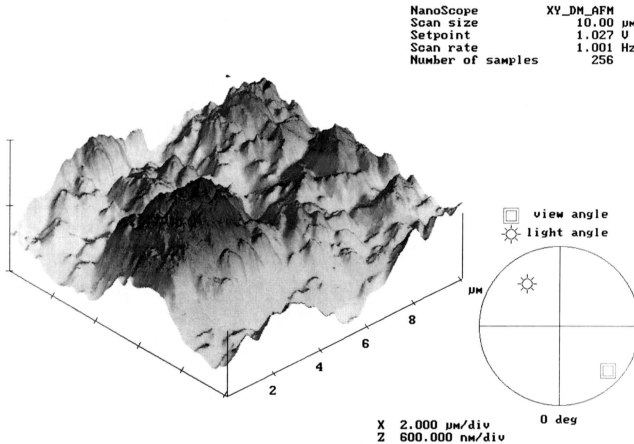

Figure 3.33 AFM scan of Zinc-Nickel deposit obtained under sonicated condition [plating current density = 1 A/dm^2]

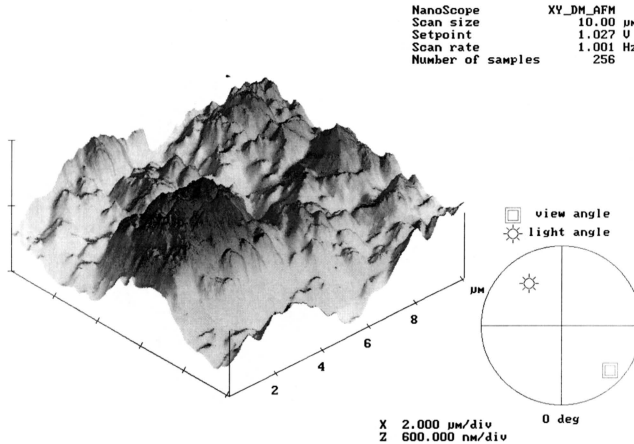

Figure 3.33 AFM scan of Zinc-Nickel deposit obtained under sonicated condition [plating current density = 1 A/dm^2]

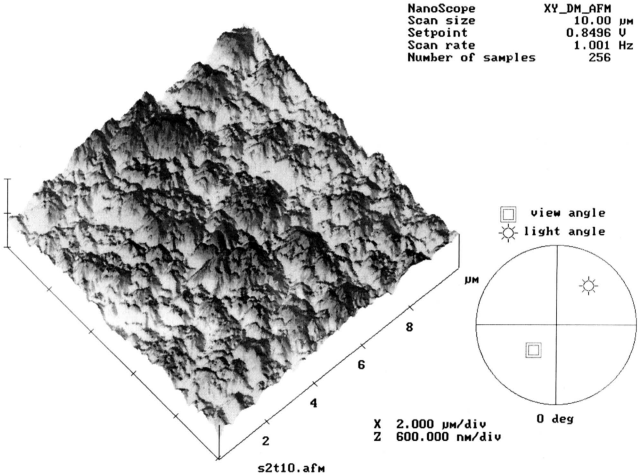

Figure 3.34 AFM scan of Zinc-Nickel deposit obtained under sonicated condition [plating current density = 2 A/dm^2]

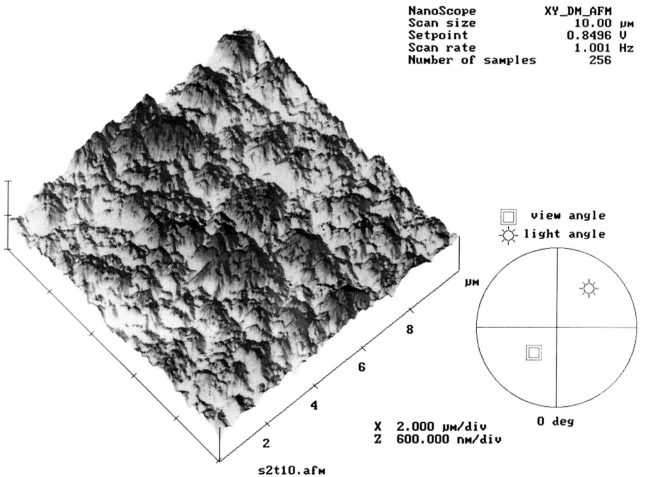

Figure 3.34 AFM scan of Zinc-Nickel deposit obtained under sonicated condition [plating current density = 2 A/dm^2]

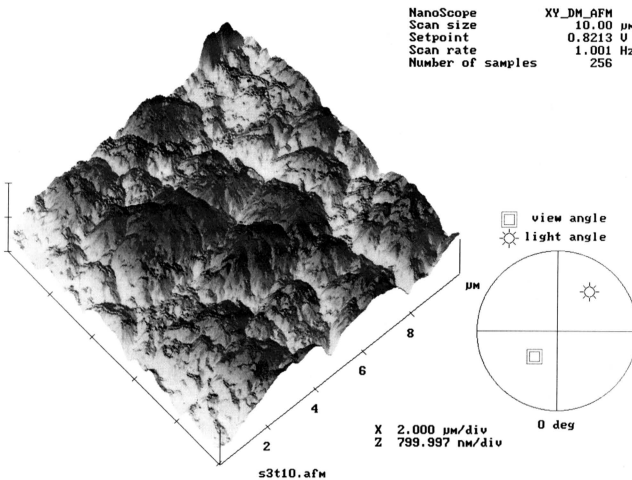

Figure 3.35 AFM scan of Zinc-Nickel deposit obtained under sonicated condition [plating current density = 3 A/dm^2]

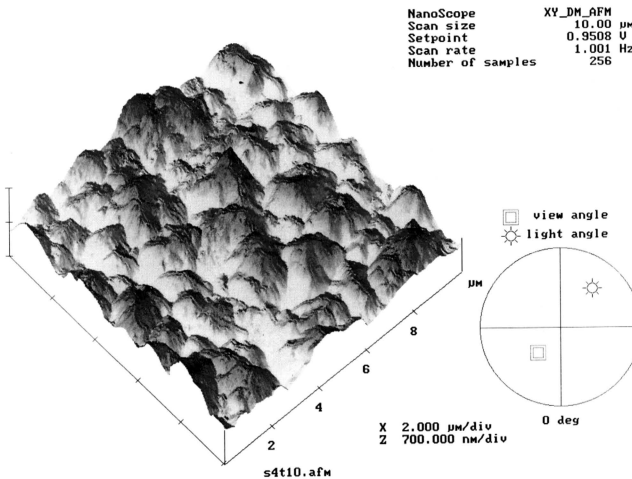

Figure 3.36 AFM scan of Zinc-Nickel deposit obtained under sonicated condition [plating current density = 4 A/dm^2]

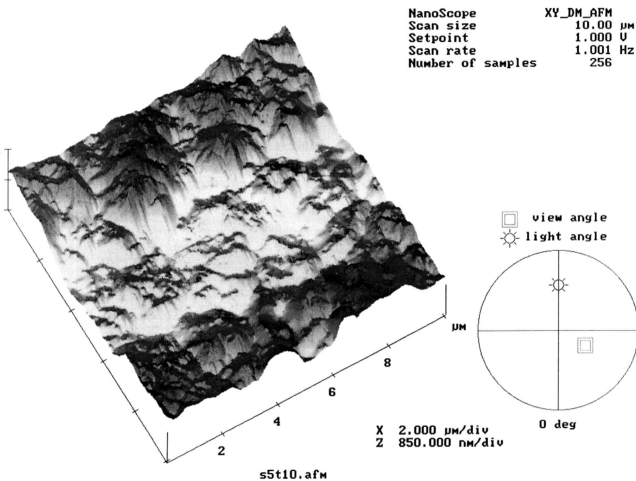

Figure 3.37 AFM scan of Zinc-Nickel deposit obtained under sonicated condition [plating current density = 5 A/dm^2]

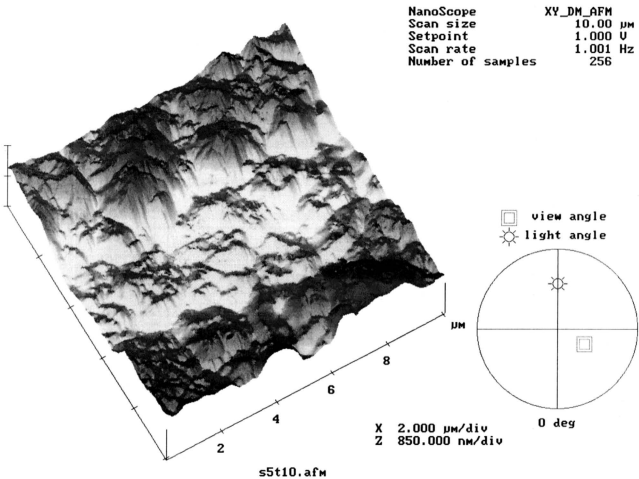

Figure 3.37 AFM scan of Zinc-Nickel deposit obtained under sonicated condition [plating current density = 5 A/dm^2]

3.5 Open circuit potential measurement

The open circuit potential of the test samples was measured as described in chapter II experimental methods. Measured potential was then converted to the half cell potential by deducting the potential of the reference electrode from the total potential so as to calculate the potential of the coating. Table 3.6 gives the potential measured for the deposits obtained under air-agitated condition.

Table 3.6 Open circuit potential of deposits obtained under air-agitated condition, after deduction of the potential of reference electrode.

Immersion time in hours	Potential (mV)				
	Plating current density (A/dm^2)				
	1	2	3	4	5
0	-865	-740	-880	-1200	-1198
2	-775	-701	-862	-1024	-1222
9	-915	-645	-835	-1132	-1066
11	-900	-906	-1004	-1186	-988
13	-907	-910	-989	-1241	-911
15	-908	-911	-975	-1223	-993
17	-909	-911	-961	-1214	-1034
19	-911	-914	-945	-1206	-1076
25	-926	-921	-921	-1102	-999
30	-934	-927	-900	-1050	-961
33	-933	-925	-915	-1024	-942
36	-933	-924	-924	-999	-923
38	-935	-925	-927	-981	-934
44	-934	-923	-941	-964	-945

Potential measured after one hour of immersion shows that the coating is less noble to that of the substrate, also there is a steady increase in the potential towards less noble direction with the increase in plating current density. Figures 3.38 shows the plot of initial potential versus the plating current density.

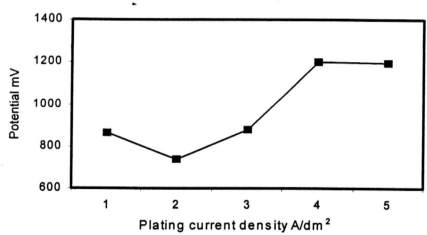

Figure 3.38 Plot of initial potential versus plating current density for the deposits obtained under air agitated condition.

The deposit obtained under plating current of $4 A/dm^2$ registered the highest potential of value -1200 mV and the potential resided well above the potential of the deposits obtained at other current densities, Indicating the maximum protection offered by the coating. Baldwin et.al. [86] reported that the initial potential tends to increase in noble direction with increase in the more noble metal (nickel) content in the deposit. The results obtained were in accordance with the observation of Baldwin. Following figure 3.39 shows the relation ship between the open circuit

potential and the nickel content in the deposit. It can be seen that at low plating current density, the concentration of nickel is high which decreases with increase in plating current density. Hence the open circuit potential of the coating tends to be less noble with increase in plating current density.

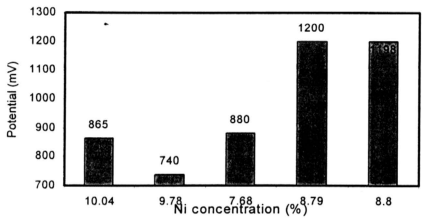

Figure 3.39 Plot of open circuit potential versus Ni concentration for the deposit obtained under air agitated condition.

Table 3.7 gives the initial potential for the deposits obtained under sonicated condition. In this case also the coating is less noble than the substrate there by behaving like a sacrificial coating.

Table 3.7 Open circuit potential of deposits obtained under sonicated condition, after deduction of the potential of reference electrode.

Immersion time in hours	Potential (mV)				
	Plating current density (A/dm^2)				
	1	2	3	4	5
0	-969	-915	-901	-917	-875
2	-921	-831	-873	-883	-861
9	-915	-675	-845	-796	-845
11	-865	-904	-970	-1073	-999
13	-980	-904	-965	-1043	-990
15	-1066	-821	-863	-1026	-984
17	-1036	-914	-957	-1015	-978
19	-965	-920	-947	-1005	-967
25	-963	-928	-920	-968	-919
30	-985	-926	-890	-931	-906
33	-975	-927	-868	-902	-908
36	-990	-928	-864	-873	-910
38	-965	-675	-775	-859	-906
44	-955	-925	-923	-857	-911

Figure 3.40 shows the relationship between the open circuit potential obtained after 1 hr of immersion and the plating current density. Figure 3.41 shows the comparison between the open circuit potential of both the air-agitated and sonicated deposits obtained after 1 hr versus the plating current density. The open circuit potential of the deposits obtained under sonicated condition remains

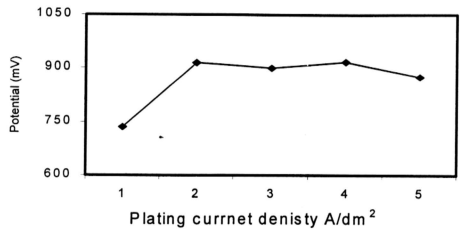

Figure 3.40 Plot of initial potential versus plating current density for the deposits obtained under sonicated condition.

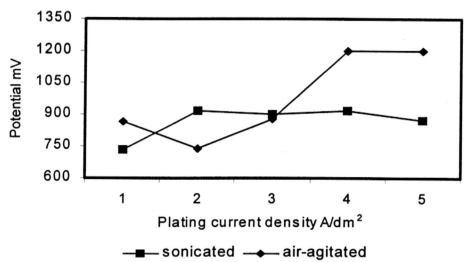

Figure 3.41 Plot of initial potential versus plating current density for the deposits obtained under sonicated condition

more or less the same when compared to the air-agitated deposits, whereas the air-agitated deposits potential increases with increase in plating current density and hence increased protection. It can be seen that the open circuit potential of the deposits obtained under sonicated condition always remains lower than the one obtained under air-agitated condition.

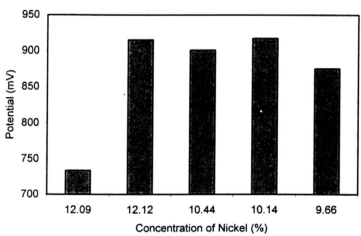

Figure 3.42 Plot of nickel concentration versus potential (mV) after 1 hour of immersion of deposits obtained under sonicated condition

In accordance with K.R. Baldwin [86] results the open circuit potential of the coating increases in less noble direction with decrease in concentration of nobler metal-nickel in the deposit as shown in figure 3.42. The basic difference between the two methods of coating arises because of the variation of concentration of the more noble metal in the

coating. Hence the coating obtained under air-agitated condition offers superior performance than the deposit obtained under sonicated condition.

The open circuit potential of the coating was followed until there is a steady value and the values obtained were plotted against time for each plating current density and for both the methods of coating. Pattern of the potential time plot of the deposits obtained under sonicated condition is entirely different from the air-agitated. The difference arises not only because of the higher or lower concentration of the nobler metal nickel in the coating but due to sonicated deposits under going different mode of crystal growth or deposition mechanism. This agrees with the observations made from the X-ray diffractograms discussed in chapter 3.1 X-ray analysis. Following figures 3.43 to 3.47 shows the potential time plot for deposits obtained under air-agitated condition at current densities 1 to $5 A/dm^2$ respectively.

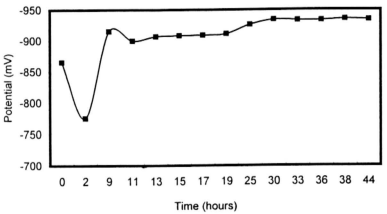

Figure 3.43 Potential versus time behaviour of the Zinc-Nickel deposit obtained at 1 A/dm^2 under air agitated condtion

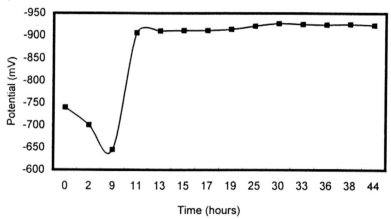

Figure 3.44 Potential versus time behaviour of the Zinc-Nickel deposit obtained at 2 A/dm^2 under air agitated condtion

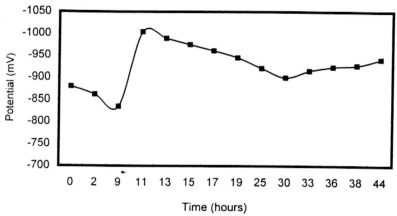

Figure 3.45 Potential versus time behaviour of the Zinc-Nickel deposit obtained at 3 A/dm^2 under air agitated condtion

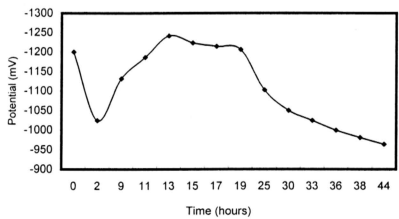

Figure 3.46 Potential versus time behaviour of the Zinc-Nickel deposit obtained at 4 A/dm^2 under air agitated condtion

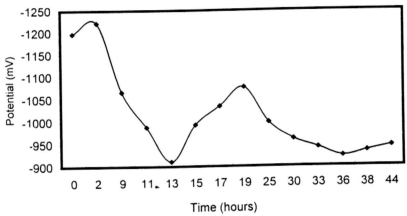

Figure 3.47 Potential versus time behaviour of the Zinc-Nickel deposit obtained at 5 A/dm^2 under air agitated condtion

As discussed earlier the initial potential of the coating remains less noble compared to the substrate, after 2 hrs of immersion the open circuit potential tends to increase in the noble direction. After that the trend changes and the coating attains the potential less noble to the substrate. The trend remains the same for all the deposits except that of the one, obtained at $5 A/dm^2$. Time taken to reach back to the open circuit potential value varies with the plating current. In the case of the deposits obtained at current densities 1 and $2 A/dm^2$ the potential after 10hrs

remains the same and attains almost a steady state value until 44 hrs. the total experiment time. Whereas the deposits obtained at plating current densities 3, 4 and $5A/dm^2$ shows a gradual increase towards the more noble direction. Indicating the increase rate of corrosion at $4A/dm^2$ with the increase in the concentration of the nobler metal nickel in the deposit.

Figures 3.48 to 3.52 shows the potential time plot for deposits obtained under sonicated condition at current densities 1 to $5A/dm^2$ respectively. By comparing the potential time plot for the air-agitated, it can be seen that the potential remains or tends to be in the noble direction indicating the less protection offered by the coating to the substrate. But in case of the sonicated deposits two depressions in the potentials were observed which could be because of the selective dezincification reported by K. R. Baldwin et.al.[86] resulting in enrichment of the metal in the coating which causes the alloy to become less active. Referring to the AFM scan's figures 3.33 to 3.37, deposition under sonicated condition results in deposition of the two metals zinc and nickel as a more homogenous individual deposits rather than resulting in a solid solution. It can be assumed that the smaller nodules found surrounding the bigger one's as nickel. This aspect is not found in the deposits obtained at 4 and $5A/dm^2$ respectively. Potential time plot of the deposits

obtained at 4 and $5 A/dm^2$ does not show any depression and the corresponding AFM scan shows a uniform deposition.

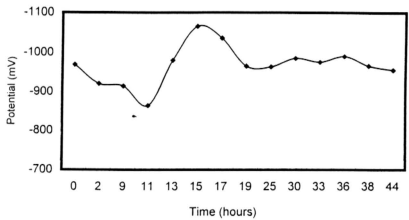

Figure 3.48 Potential versus time behaviour of the Zinc-Nickel deposit obtained at 1 A/dm^2 under sonicated condtion

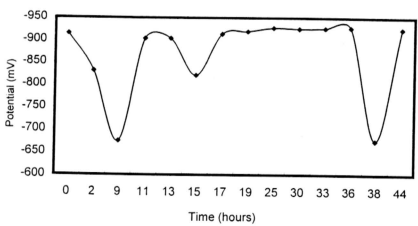

Figure 3.49 Potential versus time behaviour of the Zinc-Nickel deposit obtained at 2 A/dm^2 under sonicated condtion

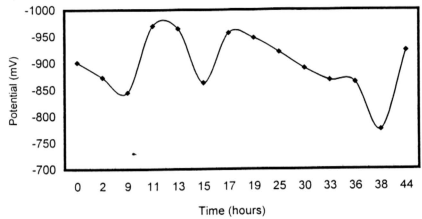

Figure 3.50 Potential versus time behaviour of the Zinc-Nickel deposit obtained at 3 A/dm^2 under sonicated condtion

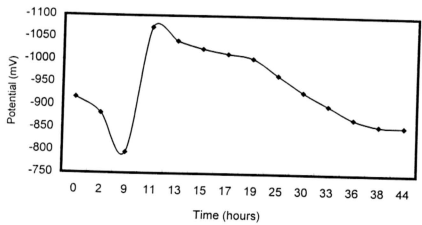

Figure 3.51 Potential versus time behaviour of the Zinc-Nickel deposit obtained at 4 A/dm^2 under sonicated condtion

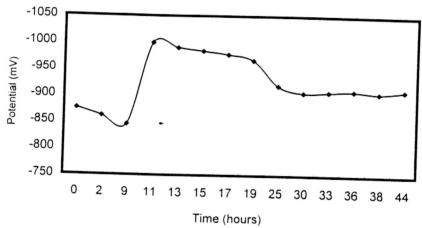

Figure 3.52 Potential versus time behaviour of the Zinc-Nickel deposit obtained at 5 A/dm^2 under sonicated condtion

Deposit obtained by sonicated method results in brighter deposits at lower current densities and turns gray in color at higher current densities with less dendrites observed at the edges.

Compared to the deposits obtained under air-agitated condition, sonication results in high concentration of nickel at any given plating current density, which inturn causes the coating to offer less protection against corrosion. Except this, all the other properties like morphology, physical appearance, integrity of the coating were much superior to the air-agitated deposits. The high concentration of nickel makes the sonication method more feasible for considering the commercial application. Lower concentration of nickel metal in the plating bath would be sufficient to get the coating of desired composition at low current density, making the environmental issues less stringent. Also, the sonication was done at 35 kHz which is on the lower side of the ultrasound, experiment should be conducted at frequencies that can result in nucleation or nebula formation, and lead to a coating which would be entirely different from the other conventional methods.